ARMA 24-0428

# The sunset solution: closure on leaking proppant

Peirce, A.P.
*Department of Mathematics, University of British Columbia, Vancouver, BC, Canada*
Abbas, S.
*SLB, Sugar Land, TX, USA*
Detournay, E.
*Department of Civil, Environmental, and Geo-Engineering, University of Minnesota, MN, USA*



**ABSTRACT:** Recent analytic work (Peirce and Detournay, 2022a) has established the tip asymptotics for receding hydraulic fractures that close due to leak-off to the permeable rock. This asymptotic result enabled the development of rigorous numerical schemes to explore the recession dynamics of hydraulic fractures that develop in a state of plane strain (Peirce and Detournay, 2022b) and radially symmetrically (Peirce, 2022). These detailed studies enabled the identification (Peirce and Detournay, 2022c) of the so-called Sunset Solution, which is a similarity solution that emerges close to the ultimate collapse of the fracture. The asymptotic analysis performed in (Peirce and Detournay, 2022c) establishes that the existence of the sunset solution is due to a fundamental decoupling of the kinematics from the dynamics in the governing equations, which leads to a robust way to measure the Carter leak-off coefficient from the rate of change in the fracture aperture at the wellbore. These results were established assuming that no fluid is leaking from the closed section of the fracture. In this paper, we explore the viability of the procedure to estimate the Carter leak-off coefficient using the sunset solution when the fracture is assumed to close on proppant that is filled with fluid upon closure and which continues to leak off and exchange fluid with the open portions of the fracture.

## 1 INTRODUCTION

The diagnostic fracture injection test (DFIT) is used in petroleum engineering to assess the minimum *in situ* stress, Carter's leak-off coefficient, and other reservoir parameters. The test consists of monitoring the well pressure during injection of fluid over a time long enough to create a hydraulic fracture, as well as after shut-in of the well. Interpretation of the pressure decline that follows the end of pumping was pioneered by Nolte (1979, 1986). His original analysis relies on two main assumptions: (i) the fracture stiffness remains constant after shut-in until the fracture completely closes and (ii) Carter's leak-off coefficient $C_L$ is a constant. In Nolte's analysis, the coefficient $C_L$ is interpreted from the pressure decline following the sudden drop of pressure observed when the well is shut-in, by expressing the declining pressure as a linear function of $G(\Delta t)$, which is a function of $\Delta t$ - the time elapsed since shut-in divided by the shut-in time $t_s$ (Nolte, 1979, 1986). This function is constructed on the assumption that the fracture growth during injection follows a power law of time. However, if the amount of fluid lost by leak-off during the propagation phase can be neglected, relative to the fracture volume, the $G$-function simplifies to $G \sim 1/\sqrt{\Delta t}$. This method to determine $C_L$ also requires an estimate of the fracture stiffness, a parameter that reflects the shape and dimension of the fracture as well as the elastic modulus of the formation. It should be noted, however, that a constant stiffness is predicated on assuming that the fracture remains everywhere open until it fully closes, a hypothesis that is not supported by numerical simulations (Wang and Sharma, 2017a). Motivated to relax some of the assumptions at the root of the original analysis, several researchers have published amendments to Nolte's interpretation of the pressure decline (McClure et al., 2016; Wang and Sharma, 2017b; Soliman et al., 2005).

The work presented in this paper to estimate $C_L$ departs from these analyses in two aspects. First, it relies on the measurement of the fracture aperture at the wellbore. Second, it is grounded on the recognition that in the last stage of closure, there is decoupling of the kinematics from the dynamics in the governing equations, with the consequence that the rate of change of the fracture aperture is simply balanced by the leak-off rate. This feature of the fracture response in the final stage of closure implies that the only information needed to determine $C_L$ is the evolution of the fracture aperture at the wellbore. This result has been proved rigorously for a penny-shaped and a KGD hydraulic fracture (Peirce and Detournay, 2022c), but on the assumption that there is no residual aperture (and thus no residual hydraulic conductivity) in the closed section of the fracture, so that fluid can only leak-off from the open part of the fracture. In reality, the fracture closes on proppant filled with fluid upon closure and the closed sections continue to leak-off and exchange fluid with the open portions of the fracture. This paper explores, via numerical simulations with the code Planar3D (Siebrits and Peirce, 2002; Peirce and Siebrits, 2001a,b), the reliability of directly estimating the Carter leak-off coefficient using the proposed approach despite the presence of proppant in the fracture.

## 2 MATHEMATICAL MODEL

### 2.1. Governing equations

The following assumptions are made in the model: (i) The fracture is assumed to be embedded in a linear elastic solid characterized by the Young's modulus $E$ and Poisson's ratio $\nu$; (ii) Fluid within the fracture is assumed to be incompressible and Newtonian with a dynamic viscosity $\mu$ while flow is assumed to be laminar and governed by lubrication theory; (iii) We consider the post shut-in dynamics of a fracture that recedes due to leak-off. By recession we mean that the fracture is closing on previously created solid surfaces at the tip; (iv) Though we primarily focus on recession, the solution at any instant depends, through the leak-off term, on the entire history of the fracture evolution from its initiation including the creation of new fracture surface. Processes that affect this history are the rate of injection $Q_0$ of a viscous fluid and the fracture the fracture toughness $K_{Ic}$, which is assumed to modulate the mode I fracture growth according to LEFM. These latter parameters determine the state of the fracture before recession starts and must be specified for completeness when presenting results.

The primary unknowns for this recession problem are the fracture aperture $w$, the fluid pressure $p_f$ or the net pressure $p = p_f - \sigma_0$, where $\sigma_0$ is the confining stress, and the fracture radius $R(t)$, which depend on the Young's modulus $E$, Poisson's ratio $\nu$, toughness $K_{Ic}$ of the solid, dynamic viscosity $\mu$ of the fluid, and Carter's leak-off coefficient $C_L$. To keep the equations uncluttered by numerical factors, we introduce the alternate parameters

$$E' = \frac{E}{1-\nu^2}, \quad K' = 4\left(\frac{2}{\pi}\right)^{1/2} K_{Ic}, \quad \mu' = 12\mu, \quad C' = 2C_L \tag{1}$$

Though we have also derived the analogous solution for a symmetric linear fracture in a state of plane strain, for the analysis presented here, we will be restricted to a radially symmetric fracture, for which the radial coordinate $r$ is confined to the interval $r \in (0, R(t))$. For the purposes of asymptotic analysis we also make use of a corresponding tip-based coordinate $\hat{r}$ (see figure 1). In the analysis presented, it is useful to define a stretched coordinate $s = r/R(t)$ and the complementary stretched coordinate centered on the tip $\hat{s} = 1 - s$. For the analysis of recession presented here, we only assume that the leak-off is described by a regular function of position and time $g(r,t)$, which does not depend on the particular form of leak-off function and does not affect the singularity of the stress field at the fracture tip. Though the asymptotic analysis and sunset solution do not rely on the form the of leak-off function, we will demonstrate how the solution obtained can be used to estimate the leak-off coefficient if Carter leak-off is assumed, in which case $g$ is given by

$$g = \frac{C'}{\sqrt{t - t_0(r,t)}} \tag{2}$$

where $t_0(r,t)$ is the first exposure time to the fracturing fluid of a fixed point on the fracture wall that is located at $r$ at time $t$. The leak-off term has a square root singularity at the tip if the fracture is propagating $V > 0$, but is finite if the fracture has arrested or is receding $V \leq 0$.

### 2.2. Receding tip asymptote

By combining Poiseuille's law and the continuity equation, we obtain the following lubrication asymptotic relation valid in the tip region $\hat{s} \ll 1$:

$$\frac{\partial \hat{w}}{\partial t} + \frac{\dot{R}}{R}\frac{\partial \hat{w}}{\partial \hat{s}} \sim \frac{1}{R^2}\frac{\partial}{\partial \hat{s}}\left(\frac{\hat{w}^3}{\mu'}\frac{\partial \hat{p}}{\partial \hat{s}}\right) - \hat{g}, \tag{3}$$

where the tip velocity $\dot{R} = V(t)$ is negative during recession and $\hat{g}(\hat{s},t)$ is the leak-off rate. After arrest, and certainly during recession, $\hat{g}$ is no longer singular as it was during propagation, and becomes more spatially uniform in the tip region, so, as time progresses, it is appropriate to assume that $\hat{g}(\hat{s},t) \sim \hat{g}_0(t)$. Though the analysis presented here applies to a radial fracture, it can be shown (Peirce

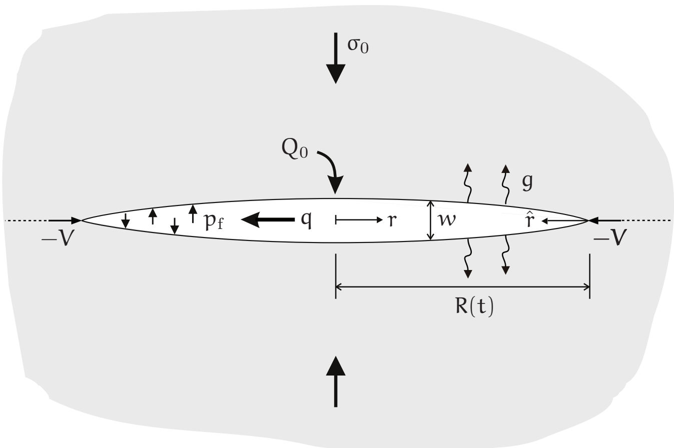


Fig. 1: Schematic of a radial hydraulic fracture that was induced to propagate by the injection of a viscous fluid at a rate $Q_0$ and which is currently receding with speed V<0.

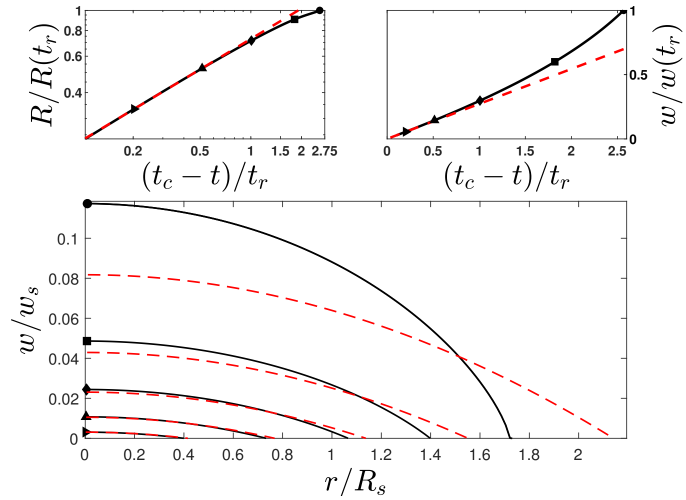

Fig. 2: Receding fracture solution (black) approaches the self-similar sunset solution (dashed red) as $t \longrightarrow t_c$

and Detournay, 2008) that the same asymptote will apply to any planar hydraulic fracture with a smooth fracture front.

We consider power-law asymptotic solutions for the fracture aperture in the tip region of the form

$$\hat{w} \overset{\hat{s}\to 0}{\sim} A(t)\hat{s}^{\lambda},\ \frac{1}{2} < \lambda \leq 1 \tag{4}$$

The lower bound restriction on $\lambda$ is required to ensure that the elastic energy release rate at the crack tip is zero for a receding fracture. The dominant behavior of the elasticity equation relating the net fluid pressure $\hat{p}$ to the fracture aperture $\hat{w}$ in the tip region can be shown (Peirce and Detournay, 2022c) to reduce to a singular integral equation with a Cauchy kernel involving $\frac{\partial \hat{w}}{\partial \hat{s}}$, which, for the power law aperture (4), has a leading behavior of the form

$$\hat{p} \sim \begin{cases} \frac{AE'\lambda}{4R}\cot(\pi\lambda)\ \hat{s}^{\lambda-1} + C,\ \frac{1}{2} < \lambda < 1 \\ \frac{AE'}{4\pi R}\ln\hat{s} + C,\ \lambda = 1, \end{cases} \tag{5}$$

where use has been made of the following identity (Peirce and Detournay, 2022c)

$$\int_0^a \frac{\hat{s}^{\kappa}}{\hat{s}-\hat{\rho}}d\hat{s} = \begin{cases} -\pi\cot(\pi\kappa)\hat{\rho}^{\kappa} + C,\ -1 < \kappa \notin \mathbb{Z}^+ \\ -\hat{\rho}^{\kappa}\log\hat{\rho} + C,\ \kappa \in \mathbb{Z}^+ \end{cases} \tag{6}$$

where $\kappa = \lambda - 1$, $\mathbb{Z}^+ = \{0, 1, \ldots\}$, and $C$ signifies that the next term is a constant, which captures the distance information in the integral implied by $a$.

Combining (3), (4), and (5) the coupled lubrication and elasticity equations reduce to the following asymptotic relation

$$\dot{A}\hat{s}^{\lambda} + \frac{\dot{R}}{R}A\lambda\hat{s}^{\lambda-1} \sim \frac{E'A^4}{\mu' R^3}\lambda(\lambda-1)(\lambda-\frac{1}{2})\cot(\pi\lambda)\ \hat{s}^{4\lambda-3} - \hat{g}_0(t) \tag{7}$$

We note from (7) that if $\lambda > 1$, the power law (4) cannot satisfy the lubrication and elasticity equations simultaneously - whence the upper bound restriction on $\lambda$ in (4). Moreover, for recession $\dot{R} < 0$, so if we assume $\frac{1}{2} < \lambda < 1$ then a dominant balance with $\hat{g}_0(t)$ is not possible since $\hat{s}^{\lambda-1}$ will become infinite. Thus, the only admissible balance is between the second and last terms in (7), which yields the linear asymptote $\lambda = 1$ and positive aperture factor $A = -R\hat{g}_0(t)/\dot{R}$, so that we obtain the linear receding asymptote:

$$\hat{w} \sim \hat{g}_0\frac{R}{|\dot{R}|}\hat{s} = \frac{\hat{g}_0}{|\dot{R}|}\hat{r},\ \text{and}\ \hat{p} \sim \frac{\hat{g}_0 E'}{4\pi|\dot{R}|}\ln\hat{r} \tag{8}$$

We also note that the first and third terms (7) match at the next order.

## 2.3. *The sunset solution*

For the numerical modeling of propagating hydraulic fractures, it has been demonstrated that making use of the tip asymptote can provide highly accurate solutions on extremely coarse meshes (Peirce and Detournay, 2008; Lecampion et al., 2013; Peirce, 2015; Dontsov and Peirce, 2017). Additionally, making use of the recession asymptote (8), it is possible to devise a rigorous and efficient numerical scheme (Peirce, 2022) that is able to capture the propagation, arrest, and recession of a post shut-in deflating hydraulic fracture. In figure 2, the black curves represent the receding fracture solution corresponding to the following values of the dimensionless parameters: $\phi^V = \left(\frac{E'^{21}\mu'^5 C'^{10} Q_0 t_s}{K'^{26}}\right)^{\frac{9}{65}} = 2$ and $\omega = \left(\frac{C'^{18}E'^4 t_s^7}{\mu'^4 Q_0^6}\right)^{1/7} = 10^{-6}$, where $t_s$ is the shut-in time. We observe that as the receding fracture approaches the collapse time $t_c$, the spatial variation of the fracture aperture becomes self-similar, while the fracture radius $R$ and aperture at the wellbore both approach power laws. To investigate the nature of this self-similar solution, we define the reverse time $t' = t_c - t$ with reference to the collapse time and observe that close to collapse, the time $t$ is assumed to be sufficiently more advanced than the leak-off trigger times active in the collapsing fracture, that the leak-off term may be replaced by the constant $g_0$.

We therefore look for a similarity solution to this "growing" (since $\dot{R}(t') > 0$) hydraulic fracture driven by an influx of fluid from a constant distributed source in terms of $s = r/R(t')$ by assuming a solution of the form

$$w(s,t') = t'^{\alpha} W(s),\ p(s,t') = t'^{\beta} P(s),\ R(t') = \Lambda t'^{\gamma} \quad (9)$$

Matching the rate of change in volume of the fracture to the leak-off rate $\dot{V}_c = (\alpha + 2\gamma)\pi\Lambda^2 t'^{\alpha+2\gamma-1}\bar{W} \sim g_0\pi\Lambda^2 t'^{2\gamma}$, where $\bar{W} = \int_0^1 W(s)s\,ds$, we conclude that

$$\alpha = 1 \text{ and } \overline{W} = \frac{g_0}{1+2\gamma} \quad (10)$$

Now in terms of the tip-centered stretched coordinate $\hat{s}$ we observe $w(s,t') = \hat{w}(\hat{s},t') = t'W(s) = t'W(1-\hat{s})$ and, because of the linear asymptote in (8), we assume a Taylor expansion for $W$ about $s = 1$ in powers of $\hat{s}$ of the form

$$\hat{w}(\hat{s},t') = t' \sum_{n=1}^{\infty} \frac{(-1)^n w_n}{n!} \hat{s}^n \quad (11)$$

where $w_n = \frac{d^n W}{ds^n}\big|_{s=1}$ and $w_0 = W(1) = 0$. Now combining (11) and (5) and using the identity (6), we obtain

$$\hat{p} \sim \frac{E' t'^{1-\gamma}}{4\pi\Lambda} \sum_{n=1}^{\infty} \frac{(-1)^n w_n}{(n-1)!} \hat{\rho}^{n-1} \log\hat{\rho}, \quad (12)$$

Comparing (12) and $(9)_b$ we observe that

$$\beta = 1 - \gamma \quad (13)$$

Moreover, using (11) and (12), we observe that the leading behavior of the flux gradient is of the form

$$\frac{1}{R^2}\frac{\partial}{\partial \hat{s}}\left(\frac{w^3}{\mu'}\frac{\partial \hat{p}}{\partial \hat{s}}\right) \sim \frac{E' t'^{4-3\gamma}}{2\pi\mu'\Lambda^3} w_1^4 \hat{s} \quad (14)$$

Since the fracture accelerates as it approaches collapse, it follows that $\gamma < 1$ so that $t'^{4-3\gamma} \ll 1$ for $t' \ll 1$, and therefore the flux gradient term on the right side of (3) becomes subdominant to the other three terms. Thus, in the limit $t' \ll 1$, there is a complete decoupling of dynamics from kinematics and (3) is reduced to a purely kinematic condition balancing fracture deflation to fluid loss.

Substituting the expansion (11) into the first two terms on the left of (3), collecting powers, and equating the result to the leak-off term $-\hat{g}$, it can be shown that there exist a countable infinity of solutions corresponding to $\gamma$ being the reciprocals of the integers $N \geq 2$, i.e. $\gamma = 1/2, 1/3, \ldots 1/N \ldots$. Now since the spatial gradient of these solutions at the fracture tip $\hat{s} = 0$ increases with $N$, it follows that the solution corresponding to $\gamma = 1/2 = \beta$ is the last admissible shape before the fracture approaches closure. Thus, the so-called sunset solution is a second degree polynomial of the form

$$w(s,t') = g_0 t'\left(1 - s^2\right),\ s = r/R,\ R = \Lambda t'^{1/2}. \quad (15)$$

A consequence of the fundamental decoupling of dynamics from kinematics is that the aperture $w$ only depends on the leak-off rate $g_0 \approx C'/\sqrt{t_c}$. Combining this with (15), it follows that the rate of change of the aperture at the wellbore ($s = 0$) as the fracture approaches collapse, yields the following estimate for $C'$:

$$C' \sim g_0\sqrt{t_c} \sim \left.\frac{dw}{dt'}\right|_{s=0} \sqrt{t_c} \quad (16)$$

### *2.4. Residual width and modeling recession using a width constraint*

Having derived the tip asymptote and the sunset solution we now discuss the numerical modeling of leak-off-driven recession by the introduction of a width constraint. For the theoretical results discussed above, the process of recession envisaged the fracture closing on previously created solid surfaces at the tip. For the analysis, we assumed that the fracture aperture was zero in the closed regions; however, the results also apply (Peirce and Detournay, 2022a) if, in the closed regions, $w = w_c$, where $w_c > 0$ is the residual aperture that may be the result of the fracture closing on proppant or asperities. In this case, the tip asymptotics and sunset solution now apply to the aperture difference field $w - w_c$. Here it has been assumed that the proppant or asperities are restricted to a constant aperture constraint. The fact that the tip asymptote and sunset solution both apply to a situation in which recession involves a fracture closing on a residual aperture opens the possibility of modeling recession by means of a minimum width constraint. Indeed, this has been how recession has traditionally been modeled (Adachi et al., 2007). However, the absence of reference solutions for recession made it difficult to determine how the magnitude of $w_c$ impacts the numerical results. The recent development of the tip asymptote (Peirce and Detournay, 2022a) and the reference solutions (Peirce, 2022), obtained from rigorous numerical schemes based on this asymptote, have made it possible to calibrate width constraint recession models (Talebkeikhah et al., 2024). This latter study also established the important result that even when a width constraint is used to model recession, the sunset solution clearly emerges.

The width constraint modeling described above does not account for the exchange of fluid between the open and width-constrained parts of the fracture or the leak-off of fluid from width-constrained regions. In this paper, we use a model (Adachi et al., 2007) that includes proppant transport, tip screenout, and closure on proppant for which the proppant concentration reaches its maximum value $c = 0.65$, as determined by the volume fraction that can be occupied by a random packing of spheres. The key elements of this model are depicted in figure 3 in which the proppant-fluid slurry is governed by Poiseuille flow in the open parts of the fracture. In regions saturated with proppant, i.e., for which $c = 0.65$, a width constraint becomes active and Darcy flow is used to describe the fluid transport through the interstitial pores formed by the packed proppant. A fluid exchange is possible across the interface between the open parts of the fracture and those parts of the fracture for which the fracture surfaces are resting on the proppant, as denoted by the black vertical line in the figure. Finally, the fluid leak-off velocity $g$ applies in the open parts of the fracture, while in the propped parts of the fracture, we assume that the leak-off velocity is $\phi_p g$, where $0 \leq \phi_p \leq 1$ is a parameter we use to be able to isolate the effect of leak-off from the propped regions. In figure 3, and subsequent aperture plots presented below, we adopt the convention of representing the open parts by the fluid (shaded green) touching the surfaces of the fracture, while the width constrained regions are represented by the proppant (shaded brown) touching the surfaces of the fracture. In the open parts of the fracture, the volume fraction of proppant in the slurry can be estimated by the ratio of the smaller brown shaded areas to those shaded green. Conversely, in the propped regions, the amount of fluid trapped in the proppant can be estimated from the ratio of the smaller green shaded areas to those shaded brown.

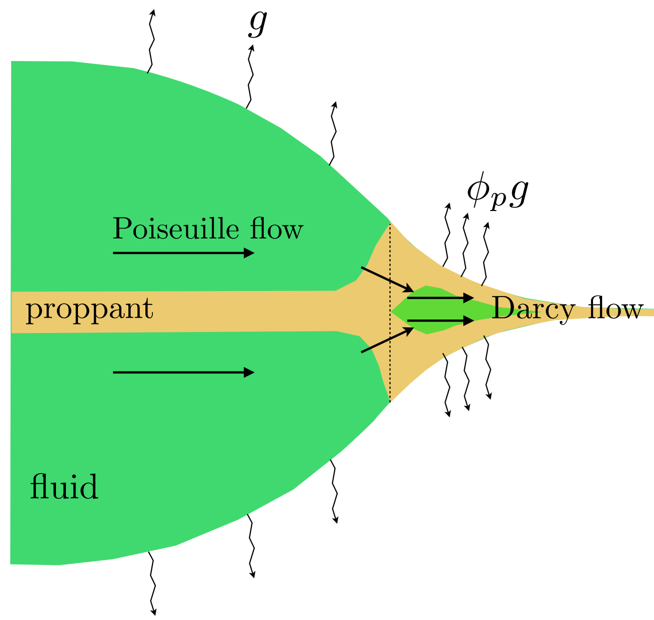

Fig. 3: Schematic of a fracture in which there is Poiseuille slurry flow that transitions to Darcy flow through the porous proppant in width-constrained regions associated with tip screenout.

## 3 RESULTS

In this section, we present results from simulations that make use of the width constraint model described in subsection 2.4. To introduce increasing levels of complexity in the models, we start with a radially symmetric fracture geometry, followed by fractures that develop asymmetrically due to jumps in the confining stress field $\sigma_0$ across horizontal interfaces. We assume that the fracture falls within the $x - y$ plane and is symmetric about the vertical $y$-axis, which coincides with the wellbore. For the geometries with vertical asymmetry, we introduce layers defined by horizontal interfaces $y_i = 490$, 500, 560, 570 m, where the wellbore is represented by a point source located at $y_s = 531$ m. In all cases, clear fluid is injected at a rate $Q_0$ until time $t_p$ after which a proppant-fluid slurry with a density $\rho_p$ is injected at the same rate until the shut-in time $t_s$. Within the proppant-packed regions, a permeability $k_p$ of loosely packed sand is assumed. In all cases, results are given for distinct values of the parameter $\phi_p$ that controls the amount of leak-off from the propped regions. The particular values of the parameters used in the simulations are provided in table 1. When there are multiple parameter values required or different parameters used for the asymmetric cases, the parameter values used for the radial cases are underlined.

### 3.1. *Radial fractures*

Figures 4, 5, and 6 all depict the results for radial fractures with the same set of basic parameters. The only difference between these figures is that the proppant leak-off factor $\phi_p = 0$, 0.5, and 1.0, respectively.

On the first row in each of figures 4-6 we plot the value of $C'$ used in the simulation (indicated by the black line) as well as the evolving estimate of $C' \sim \sqrt{t}\frac{dw}{dt}$ provided by the sunset solution (16) (indicated by the red curve) both plotted with respect to the left axis; and on the same plot, but referenced to the right axis, we plot the leak-off velocity (indicated by the blue curve). We note that this estimate

Table 1: Simulation parameters

| Parameter | Value |
|---|---|
| $E$ (GPa) | 38.7 |
| $\nu$ | 0.2 |
| $K_{\mathrm{Ic}}$ (MPa·m$^{1/2}$) | 0.01 |
| $\mu$ (Pa· s) | $\underline{1}$, 5 |
| $C_L$ (m·s$^{-1/2}$) | $\underline{2\times10^{-4}}$, $5\times10^{-4}$ |
| $Q_0$ (m$^3$·s$^{-1}$) | $\underline{0.053}$, 0.583 |
| $\rho_p$ (kg $\ell^{-1}$) | 0.12 |
| $k_p$ (m $^2$) | $1\times10^{-10}$ |
| $t_p$ $(s)$ | $\underline{1071}$, 6857 |
| $t_s$ $(s)$ | $\underline{2145}$, 10597 |
| $\sigma_0$ (MPa) | $\underline{35}$; 40; 43.5; 65 |

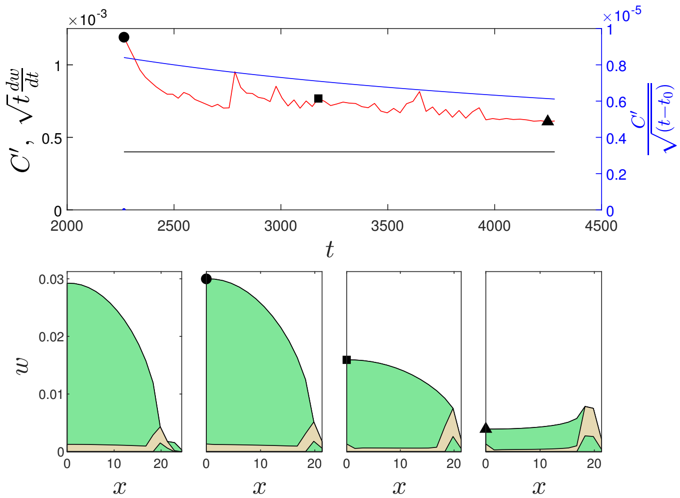

Fig. 4: Radial fracture, $\phi_p = 0$

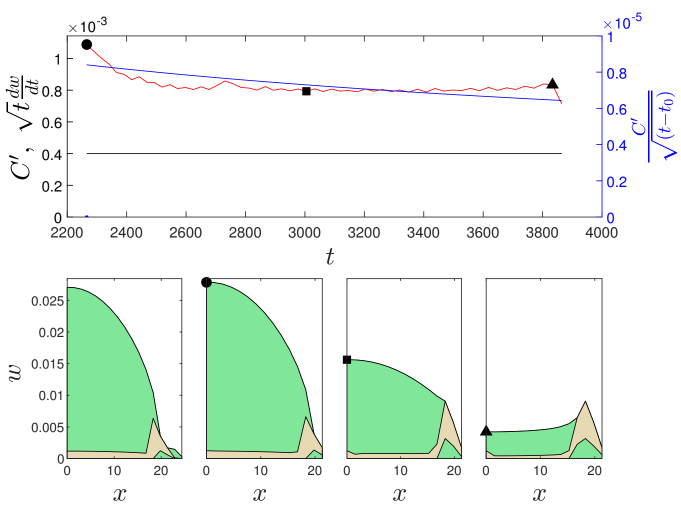

Fig. 5: Radial fracture, $\phi_p = 0.5$

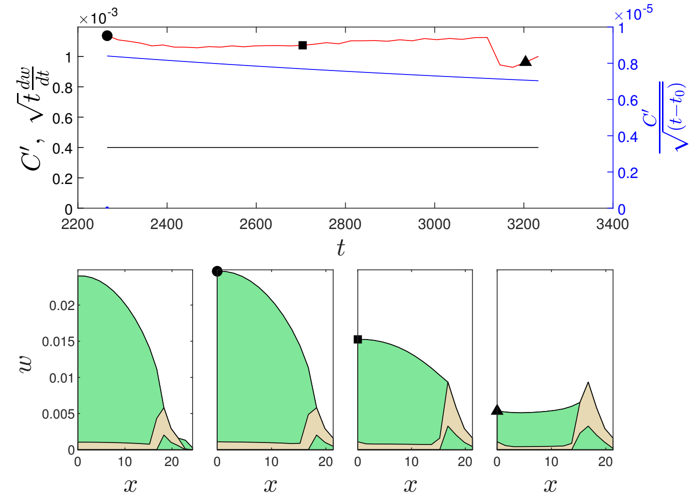

Fig. 6: Radial fracture, $\phi_p = 1$

Table 2: Sunset solution estimates of $C'$

| Geometry | $\phi_p$ | Sunset Estimate (m·s$^{-1/2}$) | Actual $C'$ (m·s$^{-1/2}$) |
|---|---|---|---|
| Radial | 0 | $6.13\times10^{-4}$ | $4\times10^{-4}$ |
| | 0.5 | $7.12\times10^{-4}$ | $4\times10^{-4}$ |
| | 1.0 | $1.0\times10^{-3}$ | $4\times10^{-4}$ |
| Stress contrast | 0 | $1.17\times10^{-3}$ | $1\times10^{-3}$ |
| | 0.5 | $1.29\times10^{-3}$ | $1\times10^{-3}$ |
| | 1.0 | $1.42\times10^{-3}$ | $1\times10^{-3}$ |

is only possible post shut-in, i.e. $t > t_s$. We also note that there is little variation in the leak-off velocity $g = \frac{C'}{\sqrt{t-t_0}}$ defined in (2). The black symbols indicated on the red curve correspond to the symbols at the wellbore for each of the post-shut-in aperture plots provided on the second row. On the second row in figure 4, we provide snapshots of the fracture aperture $w$ for the radial solution from left to right: (no symbol) this time step is chosen, sufficiently after the start of proppant injection $t_p < t_s$, that the proppant has reached the tip and screen-out has started. As a result of the tip screen-out, the aperture grows significantly as the fracture radius has ceased to grow but the fluid injection has continued; (●) just after shut-in the fracture has receded a little, but the aperture has actually increased relative to the last sampling; (■) there has been significant fluid leak-off as is evidenced by the nearly 50% decrease in the fracture aperture. There has also been a significant movement of proppant (and fluid) to the tip region as indicated by the increase in the proppant pack; (▲) similar to the previous time sample, the aperture decreases by roughly 50% again and even changes concavity, while the packed region in the tip continues to increase, a trend that is even more pronounced as $\phi_p$ increases.

Since it is closest to the assumptions under which the sunset solution was derived, the case $\phi_p = 0$ provides the best estimate of $C'$ using the sunset solution. The asymptotic estimates of $C'$ are summarized in table 2. Because there is additional leak-off from the propped tip region, which is not accounted for by the sunset solution, we would expect the estimate obtained from using the sunset solution to overestimate the value of $C'$. We would expect this overestimate even when fluid is prevented from leaking from the propped region by setting $\phi_p = 0$. This overestimate of $C'$ is caused by fluid from the open portions of the fracture being transferred to and accumulating within the proppant-filled tip region, which increases the apparent leak-off. Naturally, as $\phi_p$ increases, the overestimate becomes more pronounced. Indeed, it can be seen from table 2 that using the sunset solution overestimates $C'$ by a factor of between $1.5-2.5$ as $\phi_p$ changes from 0 to 1.

### 3.2. *Asymmetry due to a discontinuous $\sigma_0$*

In figures 7-9, we provide results for hydraulic fractures that are induced to break vertical symmetry by the discontinuous confining stress field $\sigma_0$ defined in (17). The other simulation parameters are provided in table 1, in which the parameter values not underlined are used to distinguish from the radial cases. The only difference between these figures is the different values for the proppant leak-off factor $\phi_p = 0$, 0.5, and 1.0, respectively. For ease of reference, the confining stress sequence (from bottom to top) is also provided in the figure captions.

$$\sigma_0 = \begin{cases} 35 \text{ MPa for } y < 490 \\ 65 \text{ MPa for } 490 < y < 500 \\ 35 \text{ MPa for } 500 < y < 560 \\ 43.5 \text{ MPa for } 560 < y < 570 \\ 35 \text{ MPa for } 570 < y \end{cases} \quad (17)$$

The data for this case is presented using essentially the same format as the radial case, except here a complete $y$ cross-section is provided rather than, because the symmetry of the radial case, it was sufficient to just provide cross-sections for $0 < x < R(t)$. As can be seen from these figures, the larger confining stress $\sigma_0 = 65$ MPa just below the source (whose location is indicated in the post-shut-in aperture plots by the black symbols) stops the fracture from growing into this region, while the increase in the confining stress from $\sigma_0 = 35$ MPa in the injection layer to $\sigma_0 = 43.5$ MPa in the 10 m layer just above, significantly reduces the aperture in this layer. As was observed in the radial cases, post shut-in there is a considerable decrement in aperture due to leak-off as time progresses and a redistribution of proppant from the open parts of the fracture to the tip screen-out regions, with a concomitant increase in the proppant pack. Despite the considerable deviation from the restrictive conditions under which the sunset solution was derived (both physically because of the proppant transport, tip screen-out, and width constraint modeling of deflation-recession, and because of the confining stress-induced geometric symmetry-breaking), it can be seen from table 2 that using the sunset solution overestimates $C'$ by 17 %, 29 %, and 42 % as $\phi_p$ assumes the values 0, 0.5, and 1, respectively.

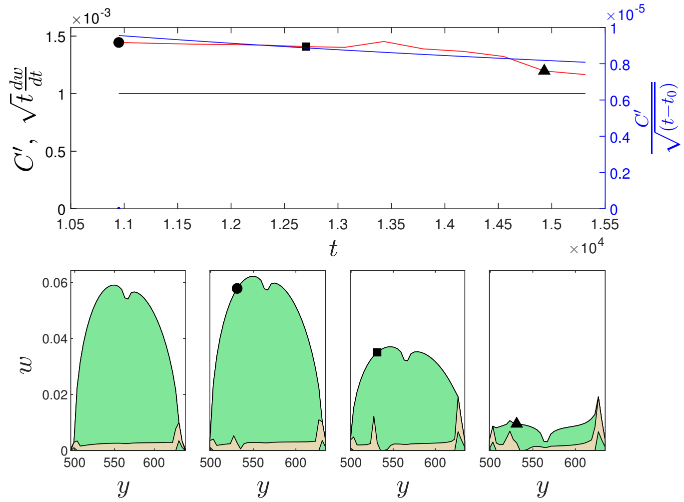


Fig. 7: $\sigma_0 = 35 : 65 : 35 : 43.5 : 35$ MPa, $\phi_p = 0$

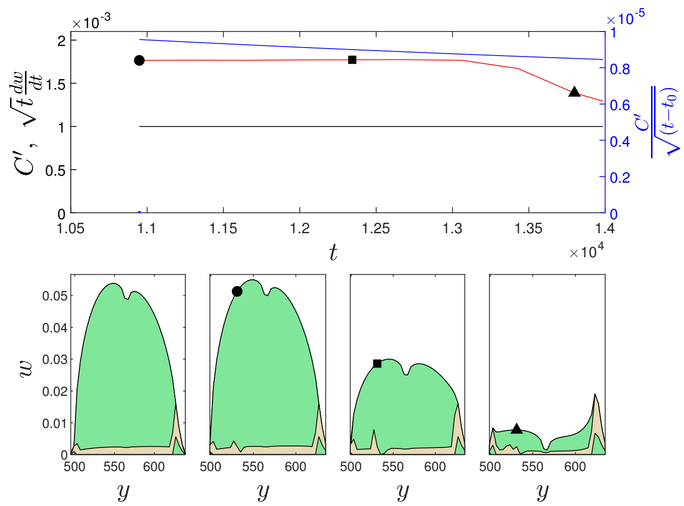


Fig. 8: $\sigma_0 = 35 : 65 : 35 : 43.5 : 35$ MPa, $\phi_p = 0.5$

## CONCLUDING REMARKS

Numerical simulations of a hydraulic fracture during the phases of fluid injection and shut-in have shown that a key result of an asymptotics analysis of a receding radial fracture (Peirce and Detournay, 2022c), namely the decoupling of the kinematics and dynamics in the governing equations before complete closure of the fracture, has more generality than expected from the assumptions used to derive this result. This decoupling leads to the important practical result that the rate of change of the fracture

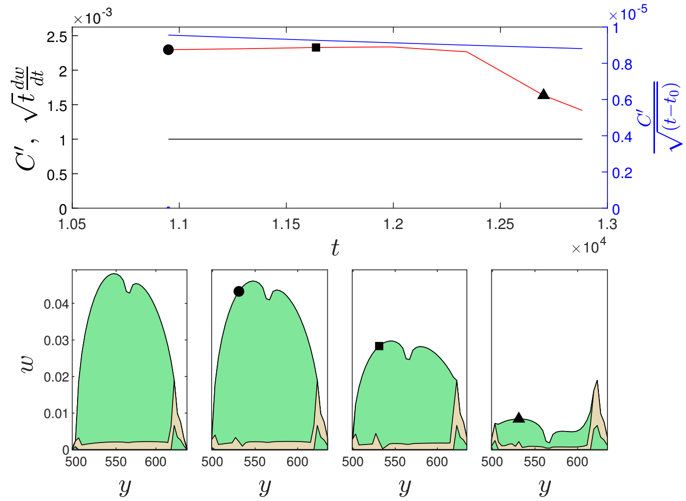


Fig. 9: $\sigma_0 = 35 : 65 : 35 : 43.5 : 35$ MPa, $\phi_p = 1$

aperture at the wellbore before complete closure, is simply equal to the leak-off rate. This result was proven on the basis of a model with a simple geometry (either plane strain or penny-shaped) built on the assumption that there is no residual aperture in the closed part of the receding fracture. However, the results of the numerical simulations presented here indicate that neither the presence of proppant in the fracture (enabling fluid to leak from the closed section of the fracture into the formation) nor symmetry breaking of the fracture geometry in the vertical direction due to jumps in the in-situ stress significantly affect the balance between the leak-off rate and the rate of change of the fracture aperture at the wellbore as the fracture is closing. This feature of the closure response of a hydraulic fracture therefore appears to be universal and not a consequence of the simplifying assumptions on the basis of which it was initially derived. This result suggests that the in-situ leak-off coefficient could be deduced from a measurement of the evolving fracture aperture at the wellbore during the last stage of closure following shut-in of the well.


## ACKNOWLEDGEMENTS

The authors would like to thank SLB for providing the computational resources required to perform the simulations and permission to use the Planar3D code. Partial support of E.D. was provided by the T.W. Bennett Chair in Mining Engineering and Rock Mechanics.


## REFERENCES


1. Adachi, J. I., Siebrits, E., Peirce, A. P., and Desroches, J. (2007). Computer simulation of hydraulic fractures. *Int. J. Rock Mechanics and Mining Sciences*, 44(5):739–757.
2. Dontsov, E. and Peirce, A. (2017). A multiscale implicit level set algorithm (ILSA) to model hydraulic fracture propagation incorporating combined viscous, toughness, and leak-off asymptotics. *Comp. Meth. Appl. Mech. and Eng.*, 313:53–84.
3. Lecampion, B., Peirce, A., Detournay, E., Zhang, X., Chen, Z., Bunger, A., Detournay, C., Napier, J., Abbas, S., Garagash, D., and Cundall, P. (2013). The impact of the near-tip logic on the accuracy and convergence rate of hydraulic fracture simulators compared to reference solutions. In A.P. Bunger, J. M. and Jeffrey, R., editors, *Proceedings International Conference for Effective and Sustainable Hydraulic Fracturing (HF2013), Brisbane, Australia*.
4. McClure, M. W., Jung, H., Cramer, D. D., and Sharma, M. M. (2016). The fracture-compliance method for picking closure pressure from diagnostic fracture-injection tests. *SPE Journal*, 21(04):1321–1339.
5. Nolte, K. (1979). Determination of fracture parameters from fracturing pressure decline. In *Proc. SPE Annual Technical Conference and Exhibition, Las Vegas*. SPE 8341.
6. Nolte, K. G. (1986). A general analysis of fracturing pressure decline with application to three models. *SPE Formation Evaluation*, December 1986:571–583. SPE 12941.
7. Peirce, A. (2015). Modeling multi-scale processes in hydraulic fracture propagation using the implicit level set algorithm. *Comp. Meth. Appl. Mech. Eng.*, 283:881–908.
8. Peirce, A. (2022). The arrest and recession dynamics of a deflating radial hydraulic fracture in a permeable elastic medium. *J. Mech. Phys. Solids*, 166:104926.
9. Peirce, A. and Detournay, E. (2022a). Multiscale tip asymptotics for a deflating hydraulic fracture with leak-off. *Journal of Fluid Mechanics*, 947(doi:10.1017/jfm.2022.623):A17.
10. Peirce, A. and Siebrits, E. (2001a). The scaled flexibility matrix method for the efficient solution of boundary value problems in 2d and 3d layered elastic media. *Comp. Meth. Appl. Mech. Eng.*, 190:5935–5956.
11. Peirce, A. and Siebrits, E. (2001b). Uniform asymptotic approximations for accurate modeling of cracks in layered elastic media. *Int. J. Fract.*, 110:205–239.
12. Peirce, A. P. and Detournay, E. (2008). An implicit level set method for modeling hydraulically driven fractures. *Computer Meth. Appl. Mech. Eng.*, 197:2858–2885.
13. Peirce, A. P. and Detournay, E. (2022b). The arrest and recession dynamics of a deflating hydraulic fracture in a permeable elastic medium in a state of plane strain. *Int. J. Solids and Structures*, 254-255:111906.
14. Peirce, A. P. and Detournay, E. (2022c). Sunset similarity solution for a receding hydraulic fracture. *Journal of Fluid Mechanics*, 944:A7.
15. Siebrits, E. and Peirce, A. (2002). An efficient multi-layer planar 3d fracture growth algorithm using a fixed mesh approach. *Int. J. Numer. Methods Engrg.*, 53:691–717.
16. Soliman, M. Y., Craig, D., Bartko, K., Rahim, Z., and Adams, D. . (2005). After-Closure Analysis to Determine Formation Permeability, Reservoir Pressure, and Residual Fracture Properties. In *Proceedings SPE Middle East Oil and Gas Show and Conference*, pages SPE–93419–MS.

17. Talebkeikhah, M., Mori, A., Lecampion, B., Peirce, A., and Detournay, E. (2024). Modeling the recession of planar hydraulic fractures by contact-based based schemes: the emergence of the sunset solution. *in preparation*.

18. Wang, H. and Sharma, M. M. (2017a). New variable compliance method for estimating in-situ stress and leak-off from dfit data. In *SPE Annual Technical Conference and Exhibition, San Antonio, Texas.* SPE-187348-MS.

19. Wang, H. and Sharma, M. M. (2017b). A non-local model for fracture closure on rough fracture faces and asperities. *J. Petr. Sci. & Eng.*, 154:425–437.